

Modeling Laryngeal Muscle: Combination of Hill-Based Active Properties with Ogden Three-Network Model

Simeon L. Smith¹, Eric J. Hunter^{1,2}

¹ National Center for Voice and Speech, The University of Utah, Salt Lake City, UT

² Department of Bioengineering, The University of Utah, Salt Lake City, UT

Presented in this technical note is the formulation of a Hill-based active stress model and its integration with the Ogden three-network passive model to model both the active and passive properties of laryngeal muscle. The goal in developing this model was to improve the muscle model used in the posturing module of the NCVS voice simulator. The complete muscle model was implemented in MATLAB and simulations were performed to compare the model behavior with laryngeal muscle. Results of the simulations are displayed, showing good agreement between the model and muscle responses. All scripts and updates to this memo can be downloaded at <http://www.ncvs.org/ncvs/library/tech>.

Keywords: Hill model, Ogden three-network model, muscle model, active/passive tissue properties, posturing, laryngeal muscle, vocal folds.

1 Introduction

Active and passive tissue properties are important to laryngeal muscle mechanics, particularly in vocal fold posturing, where the mechanical behavior of the intrinsic laryngeal muscles controls the length and medial-lateral positioning of the vocal folds. Because posturing in turn influences many aspects of voice production, including phonation pitch, threshold pressure, and voice quality^{1,2}, modeling of laryngeal muscle requires accurate definitions of both passive and active tissue properties.

In 2012, the NCVS discussed replacing the Kelvin model with the Ogden two- and three-network models in order to describe the behavior of posturing muscles in the voice simulator (see Online Technical Memo No. 14). While the Ogden model was an improvement in modeling passive tissue properties, it did not account for any active tissue properties. An active muscle stress was included by adding a constant value to the total passive stress. However, this value did not represent an accurate active stress calculation based on muscle length, contraction velocity, and activation level. A recommendation was made for integrating an active stress model into the total muscle stress equation.

In order to address the need for the inclusion of accurate active properties, a model was developed which combined a Hill-based active contractile stress calculation with the Ogden passive model already in place. This report gives the details of the active stress model and discusses the efficacy of the combined models in simulating laryngeal muscle behavior.

2 Methods

2.1 Muscle model formulation

Figure 1 shows a schematic of the mathematical muscle model, which is derived from a basic Hill muscle model³ and consists of active (top) and passive (bottom) branches. The active branch consists of a single contractile element which generates stress due to muscle activation. The passive branch is typically displayed as a spring element and uses an exponential relationship to calculate passive stress based on muscle strain (stretch). However, here it has been replaced by a schematic representing the three-network Ogden model for estimating passive properties. The total force generated in the muscle is the sum of the active stress (σ_{CE}) and passive stress (σ_{PE}):

$$\sigma = \sigma_{CE} + \sigma_{PE}. \tag{1}$$

Mechanically, the stresses are added because the elements are in parallel. In muscle modeling, this is also a generally accepted approach when the model is not mechanically based. Many studies have utilized this technique when defining active and passive properties with separate material definitions⁴. The present model follows this precedent in combining a Hill-based contractile element for the active component with a complex Ogden-based material model for the passive part.

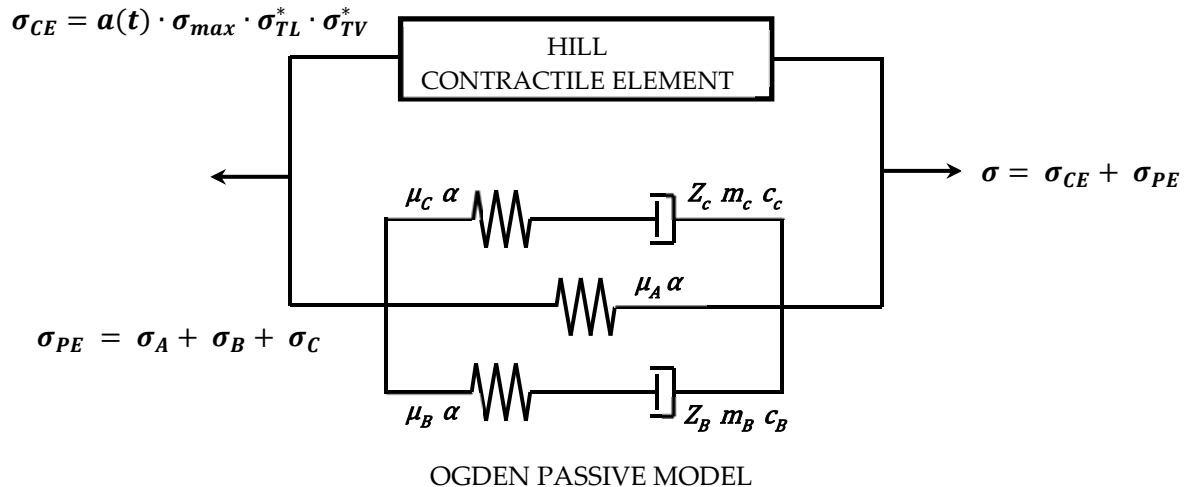


Figure 1: Schematic of muscle model. Active branch (top) consists of Hill type contractile element. Passive branch (bottom) consists of three-network Ogden model. Total stress is summation of active and passive stresses.

2.1.1 Passive properties

The calculation of passive tissue stresses was accomplished using the three-network Ogden model, which was first presented by Zhang et al.⁵ and has been used in other vocal fold modeling efforts. For a detailed description of the model, refer to Online Technical Memo No. 12 and the literature^{5,6}.

2.1.2 Active properties

As stated above, the active branch consists solely of a Hill contractile element. In finite element implementations of the Hill model, the stress due to an active muscle force can be described by the following equation:

$$\sigma_{CE} = a(t) \cdot \sigma_{max} \cdot \sigma_{TL}^* \cdot \sigma_{TV}^* \quad (2)$$

The contractile element stress magnitude is based off of σ_{max} , the maximum active muscle stress under isometric conditions and full nerve stimulation. This stress is scaled by an activation level, $a(t)$, which represents the amount of stimulation provided to the muscles by the nerves and ranges from 0 (no activation) to 1 (full or maximum activation). Further scaling is provided by the terms σ_{TL}^* and σ_{TV}^* , which are the normalized stress as functions of muscle stretch and normalized stretch rate, respectively.

Normalized stress as a function of stretch represents the dependency of force generated by the muscle on muscle length. An optimum length exists where isometric muscle stress is maximal and decreases as the muscle becomes shorter or longer. Here normalized stress is calculated as a function of stretch. σ_{TL}^* is defined by a Gaussian-type equation after Winters and Stark⁷ (Eqn. 3).

$$\sigma_{TL}^* = \exp \left[- \left(\frac{\lambda - \lambda_{opt}}{s_f} \right)^2 \right] + m\lambda \quad (3)$$

Stress is normalized by σ_{max} , and stretch is length normalized by an initial length ($\lambda = L/L_0$). λ_{opt} is the optimal stretch (at which peak stress occurs). The parameter m is a slope parameter, which is sometimes needed to capture asymmetry in the curve.

Normalized stress as a function of normalized stretch rate accounts for the dependency of muscle force on shortening/lengthening velocity. Force decreases hyperbolically as shortening velocity increases, and increases hyperbolically (but not to the same extent) as the muscle lengthening velocity increases. When velocity is zero, the force equals the isometric force as a function of length. Here force is a normalized stress and velocity is a normalized strain rate, yielding a value between 0 and 1. The hyperbolic equations used to estimate the curves for muscle contraction and lengthening, respectively, are as follows:

$$\sigma_{VL}^* = \begin{cases} a(t)\sigma_{TL}^* - \left(\frac{1 + s_p}{-s_p + \dot{\epsilon}^*} \right) \dot{\epsilon}^* & \text{if } \dot{\epsilon}^* \leq 0 \\ a(t)\sigma_{TL}^* + \left(\frac{0.4(1 + 0.5s_p)}{0.5s_p + \dot{\epsilon}^*} \right) \dot{\epsilon}^* & \text{if } \dot{\epsilon}^* > 0 \end{cases} \quad (4)$$

Here stress is normalized by σ_{max} and the muscle strain rate is normalized by the maximum muscle strain rate ($\dot{\epsilon}^* = \dot{\epsilon}/\dot{\epsilon}_{max}$).

2.1.3 Active stress response

Consideration was made for the active stress to simulate a realistic (critically damped 2nd order system) response to active stimulation. Activation level, $a(t)$, was entered into the contractile element stress calculation as a step input (immediate change in activation level and thus contractile element stress). In order to simulate the appropriate response, two coupled differential equations representing two first-order systems, each with a different time constant, were solved with the contractile element stress as the input (Eqns. 5).

$$\begin{aligned}
 t_1 \dot{\sigma}_1 + \sigma_1 &= \sigma_{CE} \\
 t_2 \dot{\sigma}_2 + \sigma_2 &= \sigma_1
 \end{aligned}
 \tag{5}$$

The output stresses, σ_1 and σ_2 , are an intermediate first-order response and final second-order response, respectively, to the contractile stress input, and t_1 and t_2 are the time constants governing the response for each system.

2.2 Model Parameter Selection

Parameters for the inputs to the active model were derived from the literature for active properties of canine cricothyroid muscles⁸⁻¹⁰. The table below lists the necessary parameters and their selected values for simulating canine cricothyroid muscle.

σ_{max}	σ_{TL}^*			σ_{TV}^*		$a(t)$	
	λ_{opt}	s_f	m	$\dot{\epsilon}_{max}$	s_p	t_1	t_2
134 kPa	1.5	0.3	0.01	2.25 l ₀ /s	0.2	0.2 s	0.8 s

2.3 MATLAB Implementation and Simulation

The active model calculations were incorporated into an existing MATLAB script for the Ogden three-network model to create a single script for the entire muscle model. The script accompanies this technical note ('Hill_Ogden_MuscleModel.m'). The scripts have all necessary sub-functions embedded. All differential equations for stress calculations are solved using a fourth-order Runge-Kutta method. Details of using the MATLAB model are given later in Section 5.

In order to compare the model response to the behavior of real muscle, simulations from the literature were replicated using the model. First, the tetanic response was simulated by applying a step activation at the beginning of the simulation. In one case, it was held throughout the simulation time, and in another case it was turned off at a given time to simulate the muscle deactivation response. These responses were compared to tests from Alipour-Haghighi et al.⁹ Next, a test of the model twitch response was performed. The muscle model was activated fully for two time durations, 2 ms and 22 ms, and the responses were compared to data from Perlman and Alipour¹¹. Finally, the muscle model was subject to a sinusoidal stretch and release, ranging

from 0% to 30% strain at a frequency of 1 Hz, the same as that performed by Alipour-Haghighi et al.⁹ Muscle and model responses were compared and are presented below.

3 Results

3.1 Tetanic response

The tetanic response of the model was compared to data for canine CT muscle presented by Alipour-Haghighi et al.⁹ Both contraction (response to activation) and relaxation (response to deactivation) were considered.

Tetanic contraction responses of the model and CT muscle are shown in Figs. 2a and 2b. Figure 2a gives normalized stress over time with activation occurring immediately at the start of the simulation, which is then held throughout. Model stress was normalized by the steady-state stress in order to compare with the already normalized muscle data. Muscle curves are shown for both the pars recta (CT-PR) and pars oblique (CT-PO) portions of CT muscle. Overall, the model response was a good fit to the literature data. The contraction time to the maximum stress matched well and the curve as it ramped up was reasonably close. There was some variation as activation initiated, particularly the model appeared to have a faster time response than the muscle, although this variation was minimal and was not much greater than the variation between the curves for the pars recta and pars oblique.

Figure 2b shows normalized stress over time compared to a different sample of CT muscle. Here activation occurred at 0.1 s and was turned off at 2.0 s. Both data sets were normalized by the maximum stress achieved. Contraction responses of the model and literature data were close again, with a seemingly identical match at the initiation of the contraction and more variation as the

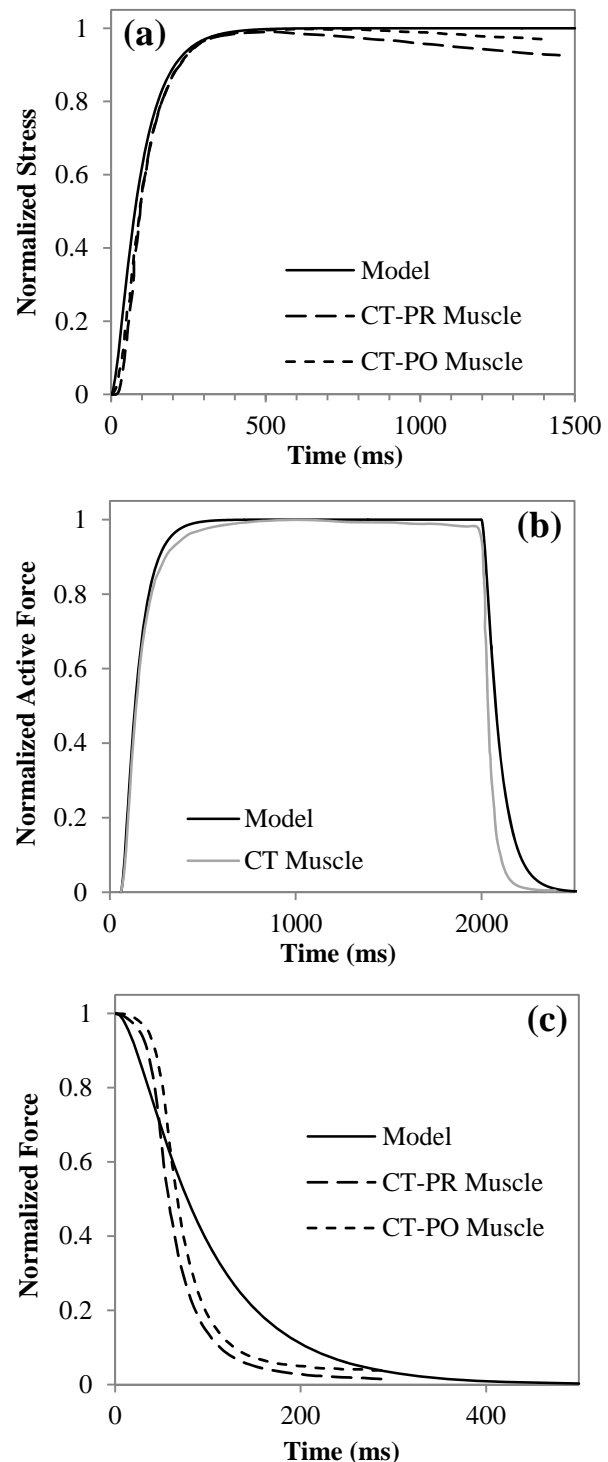


Figure 2: (a) Normalized tetanic stress response (b) Normalized tetanic force response, including contraction and relaxation (c) Normalized force resulting from tetanic relaxation. All plots show response of model compared to canine CT muscle data from Alipour-Haghighi et al.⁹

stress neared its peak. A large part of the variation was due to a longer than typical contraction time for the muscle data, which reached 90% of the maximum stress around 300 ms instead of the 200-250 ms reported as typical in literature. The maximum stress was not reached until close to 1000 ms, approximately twice that of the model contraction time.

Relaxation responses for separate samples of CT muscle are shown in Figs. 2b and 2c, plotted with the response of the model to deactivation after 2.0 sec in Fig. 2b and at the beginning of the simulation in Fig. 2c. Figure 2c gives curves for the CT pars recta and pars oblique portions. Both plots show variation between the model and muscle responses. While the model response is similar in shape to the muscle, it exhibits a sharper decrease after deactivation and the response is slower. The model has a half-relaxation time of 77 ms, whereas the muscle relaxation times are 60, 57, and 67 ms for Fig. 7 and the pars recta and pars oblique curves in Fig. 2c, respectively. Because of the mismatch in curvature, the difference continued to increase below half relaxation. Time to 90% relaxation for the model was 207 ms, which was 85 ms on average slower than that for the CT muscle samples.

Of further importance is the observation of steady-state stress over time. Figures 2a and 2b show the stress over time after maximum stress was achieved and activation was held constant. When the model transient response died out the stress remained at a constant maximum stress until some change in activation level occurred. On the other hand, the muscle stress gradually decreased over time after maximum stress was reached. This stress relaxation is typical of biological tissue. The stress typically drops exponentially and will reach an equilibrium stress eventually. The data sets from Fig. 2a showed differences of 4% and 1% between model and muscle stress for the pars recta and pars obliqua, respectively, after the first 1.0 s of tetanus (about 0.5 s at steady state). For such a short period, this difference may not be significant. However, over time the difference can become much more pronounced, and the eventual difference between the peak model stress and the muscle equilibrium stress will likely be substantial.

3.2 Twitch response

The twitch response of the muscle model was compared to a typical twitch response for laryngeal muscle from Perlman and Alipour¹¹ (Fig. 3). Perlman and Alipour provided stimulation to the muscle at 65 Hz for 2 ms. For the present study, the model was first stimulated with full activation for the same time of 2 ms. For the most part, the observed response did not compare well with the muscle data. The peak force produced by the model (about 1 gf) was only 4% of the approximately 24 gf peak of the muscle. The half-relaxation time (from peak force) of the model was 77 ms (same as with tetanic relaxation because it is dependent on system time constant), which was considerably greater than the 25 ms for the muscle.

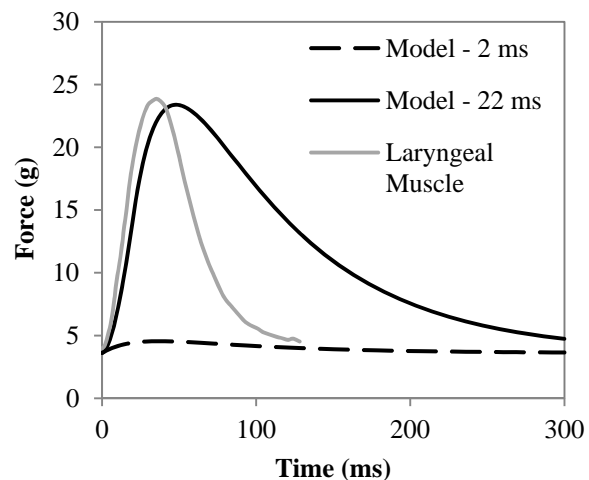


Figure 3: Muscle twitch force for two simulations with present model compared to typical twitch curve for laryngeal muscle from Perlman and Alipour¹¹.

However, twitch contraction times were close with 37 and 34 ms for the model and muscle, respectively.

More simulations were performed with the model, varying the stimulation duration in order to get a better match of peak stress. It was found that, when the model was stimulated for 22 ms, the twitch curve gave a close match for peak stress with the muscle. This curve generally had a similar shape to the twitch response of muscle. Because the activation duration was increased the response had a longer contraction time (48 ms), and half-relaxation time was still 77 ms.

3.3 Sinusoidal strain

Depicted in Fig. 4 is the model stress resulting from a sinusoidal strain input with activation, compared to the same simulation performed on CT muscle by Alipour-Haghighi et al.⁹ The muscle was fully activated at 1.75 s, thus resulting in only passive stress for the first half of the simulation and combined passive and active for the latter half. Overall, the curves were remarkably similar. Shapes and amplitudes of each oscillation were generally the same. Peak stresses matched, both for passive only (first peak) and passive and active combined (third peak).

The present model response did differ somewhat from the muscle response. Much of the dissimilarity was due to differing levels of stress relaxation. While the model predicted the first passive peak stress well, the peak stress during the second oscillation had decayed more in the model than in the muscle. If these stress relaxation rates matched up the third peak stress would actually have been over-predicted by the model since the passive contribution would not have decayed as much. Active stress does not decay, and toward the end of the simulation the passive stress relaxation started to steady out so that it was minimal, causing the fourth peak stress to be greater for the model than the muscle. Other small variations between the data sets existed, particularly as stress increased. The model had a faster response when only passive stress was present and a slightly delayed response with activation. The greatest variation was seen on the upslope of the third peak as activation started. The fourth peak might have shown similar variation if the peak stresses were equal. Passive stress downslopes also showed slight variation between the model and muscle curves.

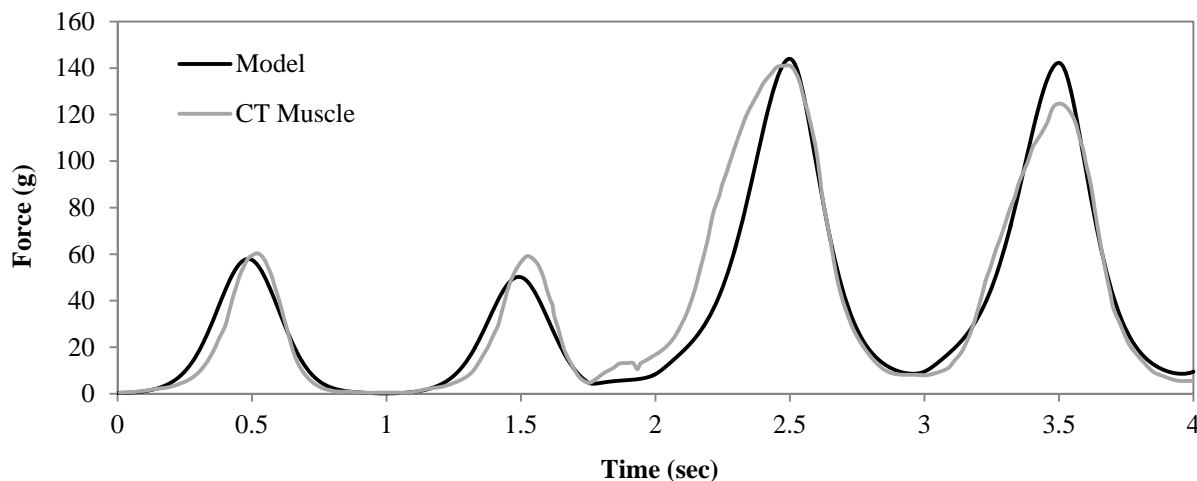


Figure 4: Model force compared to CT muscle force presented by Alipour-Haghighi et al.⁹, in response to sinusoidal strain with activation after 1.75 sec.

4 Conclusions and Future Work

A new muscle model with accurate passive and active properties was examined. The results overall suggest that the combination of the three-network Ogden model and a Hill-based active model estimates well the passive and active stresses of muscle during both isometric and dynamic conditions. In comparison to isometric tetanic contraction of CT muscle, the model stress response showed appropriate contraction times and matching curvature. Tetanic relaxation and twitch responses were also similar to those exhibited by real muscle. Furthermore, the model provided an excellent approximation of the muscle force (stress) behavior resulting from dynamic stretch and release with activation, as compared to published data for canine CT muscle.

As well as the new model being an accurate representation of muscle behavior, it appears to be a viable improvement to the posturing model. By including a Hill-based active stress in the muscle model, the stress fluctuations that were seen when an arbitrary active stress was simply added into the total stress are eliminated. Thus, the new model has no unexplained numerical errors, and is stable and robust for the desired range of input values. Additionally, because it solves the active and passive stresses separately, the accuracy of the passive model is not affected. Moreover, the active stress calculations are simple, discrete, and are not computationally expensive, making this model easy to implement into finite element code.

In the future, work should be performed to implement and improve the muscle model. The main upcoming goal is to utilize it in the posturing model of the voice simulator. For this, the MATLAB code must be converted to FORTRAN and integrated with the other simulator modules. Also of importance would be to further validate the model by comparing to experimental data for other muscles and simulations, and to improve limitations of the model such as adding an active stress decay.

5 Using the Current MATLAB Model

This section demonstrates how the MATLAB script ('Hill_Ogden_MuscleModel.m', provided with this report) was used to perform the simulations, obtain the response data, and create the figures associated with this report. The information provided should enable the reader to navigate, adapt, and run simulations with the muscle model.

All of the simulations were run and data obtained using the same script with different inputs. The varied inputs included the prescribed muscle strain, simulation time, and the activation level as a function of time. Muscle strain was defined with the variables `eps_amp` (strain amplitude in %) and `eps_` (strain at each time step) in lines 56-57 of the script. For the tetanus and twitch responses, both variables were set to zero for 0%, while the cyclic strain simulation employed the following sinusoidal function to define strain: $\text{eps_amp}/100 * (1 - (0.5 + 0.5 * \cos(2 * \pi * \text{time_} * \text{freq_})))$. Simulation time (variable `time_`) was set in line 55. Activation level as a function of time was expressed with the variables `a_1` (activation level magnitude, line 73) and `act` (level at each time step, lines 77-78). For all the simulations here, full activation was used (i.e., `a_1 = 1.0`) and the activation period was given for each simulation by varying `act`.

The response data (output stresses) were exported from MATLAB and imported into Excel to create the plots shown here. Lines 125-128 of the code write the output stresses to a text file. The name of the output file was varied to differentiate the simulation outputs. Each text file and the

corresponding literature data (extracted from the published plots using a plot digitizer) were copied to an Excel spreadsheet and plotted for comparison. It should be noted that the script does create various output plots (lines 135-155) which can be included or commented out by the user. It was possible to create the results plots here via MATLAB. However, Excel was chosen to facilitate the combination of the two data sets (model and literature) and for ease of formatting.

In addition to setting the desired simulation parameters and plotting options, the user can further adapt the model to represent muscle properties other than the canine cricothyroid muscle. This can be accomplished by altering the active muscle model parameters and time constants in lines 67-72 and 44-45 of the code, respectively. After the inputs and outputs have been defined, the simulation is executed by typing the function name into the MATLAB command line or by simply running the script from the editor window.

Acknowledgements

Funding for this work was provided in part by the National Institute on Deafness and Other Communication Disorders, grant number R01 DC006101, (P.I.) Roger W. Chan (“Biomechanical characterization of vocal fold tissues”).

Literature

- (1) Titze IR. The physics of small-amplitude oscillation of the vocal folds. *J Acoust Soc Am* 1988; 83:1536-1552.
- (2) Murry T, Xu JJ, & Woodson GE. Glottal configuration associated with fundamental frequency and vocal register. *J Voice* 1988; 12:44-49.
- (3) Hill AV. The Heat of Shortening and the Dynamic Constants of Muscle. *Proc R Soc Lond* 1938; 126:136-195.
- (4) Hedenstierna S, Halldin P, and Brolin K. Evaluation of a combination of continuum and truss finite elements in a model of passive and active muscle tissue. *Comp Methods Biomech Biomed Eng* 2008; 11:627-639.
- (5) Zhang K, Siegmund T, Chan RW, Fu M. Predictions of fundamental frequency changes during phonation based on a biomechanical model of the vocal fold lamina propria. *J Voice* 2009; 23:277-282.
- (6) Chan RW, Siegmund T, Zhang K. Biomechanics of fundamental frequency regulation: Constitutive modeling of the vocal fold lamina propria. *Logoped Phoniatr Vocol* 2009; 1-9.
- (7) Winters JM & Stark L. Analysis of fundamental human movement patterns through the use of in-depth antagonistic muscle models. *IEEE Trans Biomed Eng* 1985; 32:826-839.
- (8) Titze IR. *The Myoelastic Aerodynamic Theory of Phonation*. National Center for Voice and Speech, Iowa City. 2006.
- (9) Alipour-Haghighi F, Perlman, AL, and Titze, IR. Tetanic response of the cricothyroid muscle. *Ann Otol Rhinol Laryngol* 1991; 100:626-631.
- (10) Alipour F, and Titze I. Active and passive characteristics of the canine cricothyroid muscles. *J Voice* 1999; 13:1-10.
- (11) Perlman AL & Alipour-Haghighi F. Comparative study of the physiological properties of the vocalis and cricothyroid muscles. *Acta Otolaryngol (Stockh)* 1988; 105:372-378.

Copyright

The images and text are open to use by the public as a service of the National Center for Voice and Speech. However, we ask the reader to respect the time and effort put into this manuscript and research. If the text, images, or included scripts are used, the user agrees to reference to this document and the National Center for Voice and Speech. We reserve the right of refusal to (1) be authors on papers using the device and scripts and (2) have the supporting project acknowledged. The user agrees to freely share with the NCVS any extension software build on the scripts contained.

Content Note

Some of the figures are also part of a manuscript under review in a peer review journal. When that manuscript is published, this technical note will be modified to acknowledge that work, as well as provide supplemental materials like the MATLAB script.

Revisions

1.0 Simeon L. Smith: Main document with edits from Eric Hunter (March 2013)